ELSEVIER

International Journal of Mass Spectrometry 223–224 (2003) 771–782

International Journal of Mass Spectrometry

www.elsevier.com/locate/ijms

Atmospheric pressure chemical ionization mass spectrometry for the detection of tropospheric trace gases: the influence of clustering on sensitivity and precision

C. Jost*, D. Sprung[1], T. Kenntner, T. Reiner[2]

Biogeochemistry Department, Max Planck Institute for Chemistry, P.O. Box 3060, 55020 Mainz, Germany

Received 23 July 2002; accepted 30 July 2002

Abstract

An atmospheric pressure chemical ionization mass spectrometer (AP-CIMS) was set up for the detection of the atmospheric trace gases acetonitrile, acetone, and sulfur dioxide. This instrument, which was successfully employed in several, mainly airborne, field campaigns, is described in detail. The ion source makes use of a corona discharge at near ambient pressure. Acetonitrile and acetone are detected as protonated species after undergoing ligand-switching reactions with ions which have an H_3O^+ core. Sulfur dioxide is detected as SO_3^- produced in a reaction with CO_3^-. The instrument is calibrated using permeation tubes. The instrument response was found to be highly sensitive to the sample humidity. This is accounted for by applying a humidity dependent calibration; the AP-CIMS itself is used to measure the humidity. The detection limits are 10, 20, and 80 ppt for acetonitrile, sulfur dioxide, and acetone, respectively. The analytical precision for all three measured compounds is 18% or better for typical conditions and for an integration time of 3 s. Dimethylsulfide and methyl mercaptan were found to be potential interferents, probably due to radical chemistry in the ion source region. This restrains the applicability of this technique for sulfur dioxide measurements to regions with low dimethylsulfide and methyl mercaptan concentrations, i.e., outside the marine boundary layer. (Int J Mass Spectrom 223–224 (2003) 771–782)

Keywords: Atmospheric pressure chemical ionization mass spectrometry (AP-CIMS); Tropospheric chemistry; Cluster ions; Humidity interference

1. Introduction

In an atmospheric pressure chemical ionization mass spectrometer (AP-CIMS), also called ion–molecule reaction mass spectrometer (IMRMS), reactant ions, $A^{\pm}$, are produced in an ion source. These ions can react with trace gas molecules, X, present in the sample, and produce new ions, $B^{\pm}$, according to

$$A^{\pm} + X \xrightarrow{k} B^{\pm} + Y \quad (1)$$

where k is the rate coefficient. These reactions take place at approximately atmospheric pressure to achieve a high collision rate and, thus, a high sensitivity. The AP-CIMS technique also causes relatively little fragmentation, facilitating the interpretation of measurements in a complex mixture such as air.

* Corresponding author. E-mail: jost@mpch-mainz.mpg.de
[1] Present address: Institute of Climate Research and Meteorology, Research Center Karlsruhe, Karlsruhe, Germany.
[2] Present address: Endress + Hauser GmbH & Co., Weil am Rhein, Germany.

1387-3806/02/$ – see front matter
PII S1387-3806(02)00963-6

The use of mass spectrometric techniques for atmospheric chemical studies was pioneered by Arnold et al. [1] and Eisele [2], who analyzed naturally occurring ions in the atmosphere. These measurements were the starting point for the AP-CIMS technique, which has been employed to detect compounds such as acetone and other volatile organic compounds (VOCs), nitric acid, sulfur dioxide, sulfuric acid, organic sulfur compounds, and, using indirect techniques, HO_x [3–9].

We employed an AP-CIMS instrument to detect acetone (CH_3COCH_3), acetonitrile (methyl cyanide, CH_3CN), and sulfur dioxide (SO_2) on several aircraft campaigns, namely, INDOEX (Maldives, 1999) [10–12], INTACC (Sweden, 1999) [13,14], and SAFARI 2000 (Namibia, 2000) [15]. Measurements of these compounds were complicated by clustering reactions that make the sensitivity of the instrument depend on ambient humidity. We used a novel method to take these effects into account. This method is based on a humidity dependent calibration, for which the mass spectrometer itself is used to determine the humidity.

2. Methods and experimental

2.1. The instrument

A scheme of our instrument is shown in Fig. 1. The instrument is manufactured by ABB Extrel, Pittsburgh, Pennsylvania, USA. The ion source makes use of a corona discharge. It is run at a voltage of typically 5 kV DC and the current is limited to ∼5 μA by a resistor of 1000 MΩ. The corona discharge burns between a needle and the aperture lens.

The sample gas passes through the ion source. In the ion source region the ion–molecule reactions according to Eq. (1) take place. This region is kept at a temperature of 80 °C and a pressure of 280 hPa. To achieve this pressure, the sample flow is regulated by a control valve. This pressure is chosen to be lower than the pressure in the aircraft sampling line to ensure that it is constant even under these special circumstances.

The ion source region is separated from the decluster chamber by the aperture lens, which has an orifice of 0.25 mm in diameter. About 0.2 sL min^{-1} (standard

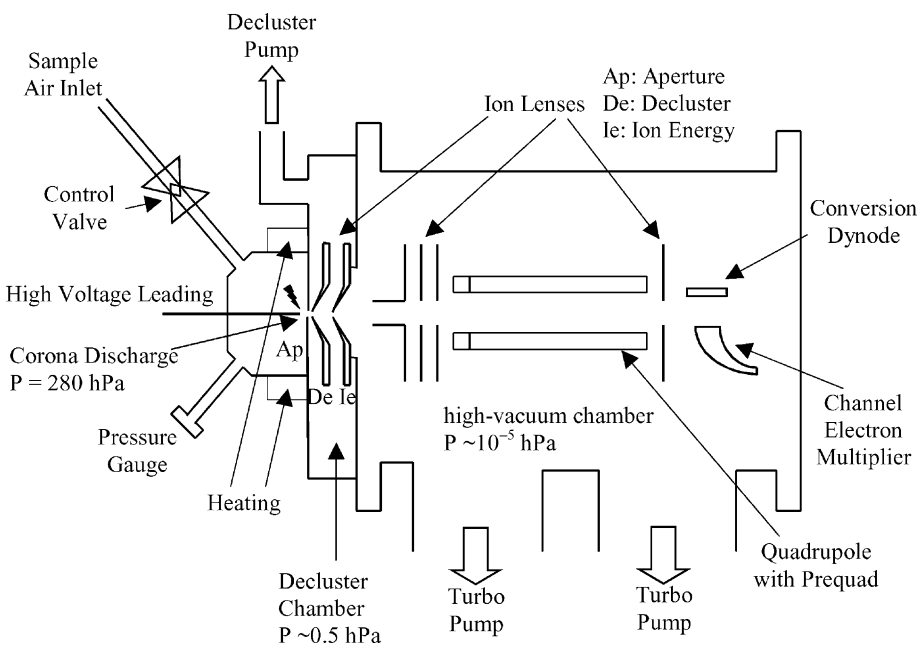

Fig. 1. Scheme of the instrument used in this work.

liter per minute) sample air are drawn through the ion–molecule reaction chamber and the aperture lens. Downstream of the aperture lens the pressure is reduced to 0.5–1.0 hPa in the decluster chamber, which is still sufficient for collisions to take place.

The ions enter the high-vacuum chamber through the ion energy lens in a flow of remaining neutral gas at $\sim 10^{-3}$ sl min^{-1}. In the high-vacuum chamber, there is a lens system to improve the transmission, a quadrupole rod system, and a channel electron multiplier to detect the ions. The pressure in the high-vacuum chamber is about 10^{-5} hPa, which results in a mean free path length of several meters. Two turbo molecular pumps that are backed by a rotary vane pump produce the high vacuum.

2.2. Ion evolution

The corona discharge ionizes initially mainly the most abundant gases oxygen and nitrogen. The ions formed are the starting point for cascades of ion–molecule reactions, which occur similarly in the atmosphere [16]. After ~ 1 μs positive charged ions are mainly $H_3O^+(H_2O)_n$ (see Fig. 2a and b). For negative

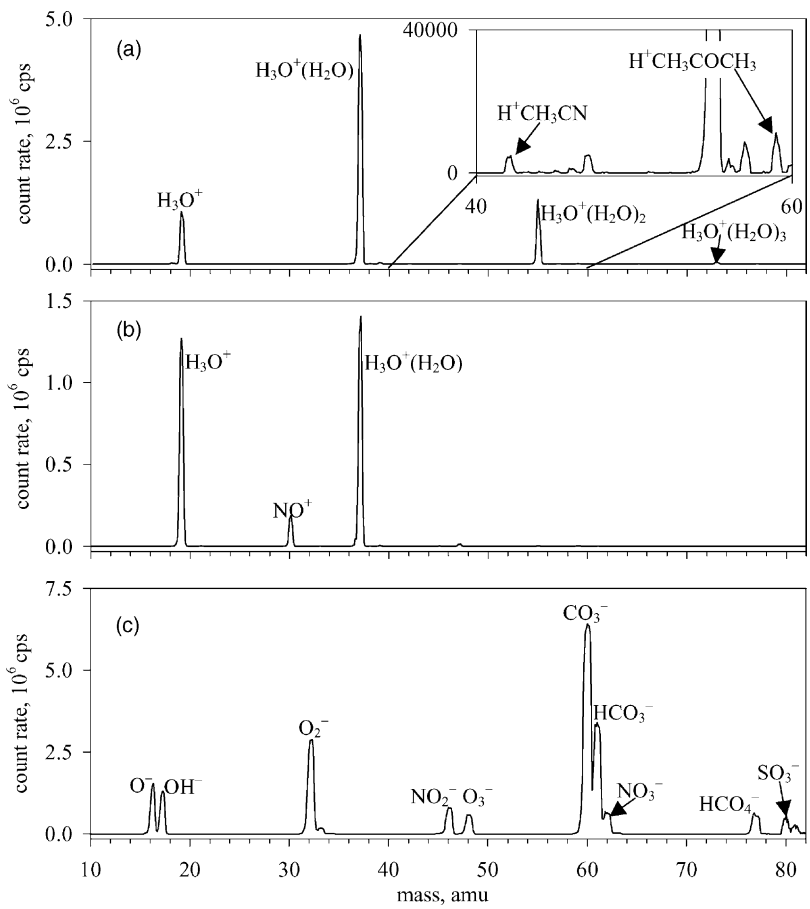

Fig. 2. (a) Spectrum of positive ions at high humidity for a calibration run, obtained in a cloud layer at 550 m altitude over the South Atlantic Ocean near the Namibian coast on 7 September 2000. (b) Spectrum of positive ions under dry conditions, obtained at 5700 m altitude over Namibia on 16 September 2000. (c) Spectrum of negative ions for a calibration run, obtained at 1000 m altitude over the South Atlantic Ocean near the Namibian coast on 14 September 2000; masses from 79.5 amu on are scaled up by a factor of 100, mass 80 amu is enhanced due to a calibration with about 4 ppb sulfur dioxide.

spectra, O^-, O_2^-, OH^-, NO_2^-, O_3^-, CO_3^-, HCO_3^-, NO_3^- and HCO_4^- ions can be observed (see Fig. 2c).

H_3O^+ $(H_2O)_n$ can undergo ligand-switching reactions with trace compounds which have a higher gas phase basicity than water, such as acetonitrile or acetone [17,18]:

$$H_3O^+(H_2O)_n + CH_3CN \rightarrow H^+CH_3CN(H_2O)_n + H_2O \quad (2)$$

$$H_3O^+(H_2O)_n + CH_3COCH_3 \rightarrow H^+CH_3COCH_3(H_2O)_n + H_2O \quad (3)$$

Several negative ions can undergo reactions with SO_2, leading to the formation of SO_3^-. Of these, CO_3^- are the most important ones [4,19,20]:

$$CO_3^-(H_2O)_n + SO_2 \rightarrow CO_2 + (n-m)H_2O + SO_3^-(H_2O)_m \quad (4)$$

The product ions of reaction (2)–(4) are indicated in Fig. 2.

Eqs. (2)–(4) can be understood as representations of the general Eq. (1). The analysis of the kinetics of these reactions allows at first approximation, to quantitatively analyze the trace compounds involved in the ion–molecule reactions. The integration of the kinetic equation and linear approximation of the logarithm function leads to Eq. (5) for the concentration of X in Eq. (1) of the neutral trace gas

$$[X] = \frac{1}{k\tau}\frac{[B^\pm]_{t=\tau}}{[A^\pm]_{t=\tau}} \quad (5)$$

where τ is the reaction time, which is ~60 μs for our instrument, and $[A^\pm]$ and $[B^\pm]$ are the concentrations of the ions $A^\pm$ and $B^\pm$ which are detected by the mass spectrometer. According to Eq. (5), $[X]$ is proportional to the count rate ratio of product ions $B^\pm$ to reactant ions $A^\pm$. The quantity $1/k\tau$ can be determine by performing calibrations or by calculating it from the reaction time τ and the effective rate coefficient k for the respective reaction. We chose the former to avoid the uncertainties associated with the effective rate coefficient (see Section 3.2).

3. Results and discussion

3.1. Linearity

The theoretically linear relationship between $[X]$ and the count rate ratio of $B^\pm$ to $A^\pm$ was investigated in multi-point calibrations. The linear correlation was nearly perfect for acetonitrile and acetone with squared correlation coefficients $r^2 = 0.999$ for both compounds (see Fig. 3), and good for sulfur dioxide with $r^2 = 0.989$. Thus, errors resulting from a potentially non-linear response of the instrument in the relevant range are ~1% or better.

3.2. Clustering reactions

As indicated in Eqs. (2)–(4), product ions can occur with different numbers of water molecules attached to them. Additionally, an oxygen molecule can attach to a SO_3^- core ion and form a SO_5^- ion [19]. These clustering reactions make the signals of the product ions shared by many masses and can lead to interferences. This can be avoided by collision-induced dissociation in a decluster chamber (see Fig. 1). The decluster chamber is usually employed at a pressure of 0.5–1 hPa, where the gas particles have typical free mean path lengths of 50–100 μm. The ions can be accelerated in the electric field between the lenses to control the energy of the collisions causing the declustering [21]. In Fig. 2a signals from $H_3O^+(H_2O)_n$ ions with $n = 0$ to 3 are shown. In a humid environment, also a small signal on mass 91 amu from $H_3O(H_2O)_4$ can be observed, indicating that the declustering is not complete, but no signals from clustered product ions could be found in the calibrations, similar to the findings of Sunner et al. [22].

Clustering affects the sensitivity of the instrument and causes, therefore, a humidity dependence. The sensitivity of our instrument varies up to an order of magnitude for extremely different conditions. The sensitivity can be influenced in two different ways. First, the rate coefficient of the ion–molecule reactions can depend on the number of water molecules clustered to the primary ions; second, reverse reactions can lower

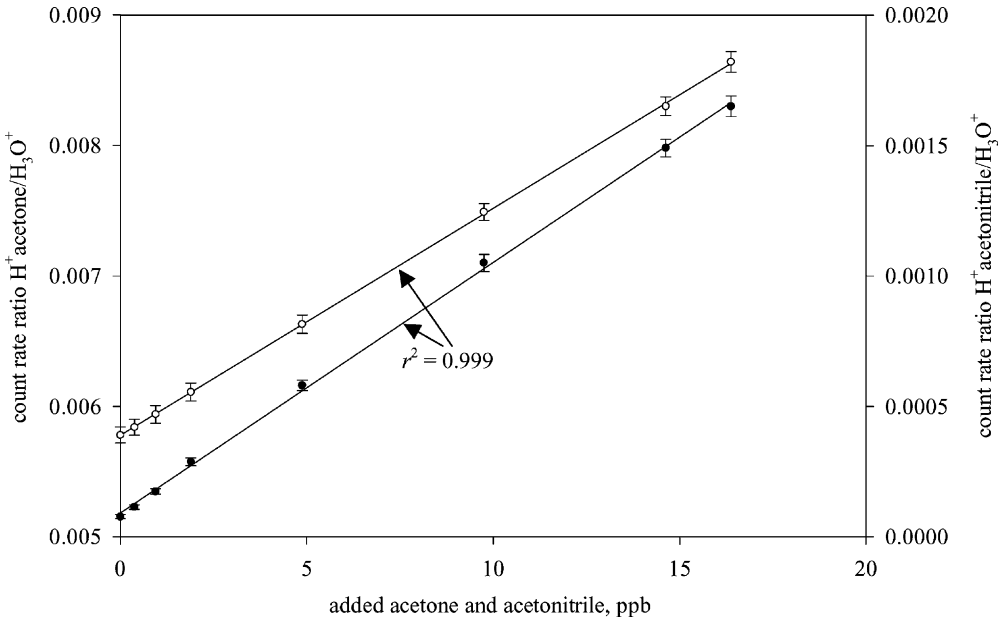

Fig. 3. Multi-point calibration for acetonitrile and acetone and linear regressions. The error bars represent the standard deviation for the measurement time of 2 min. The calibration gas was added to laboratory air. The relatively large background signals, especially for acetone, are due to the enhanced concentrations in the laboratory.

the product ion to reactant ion ratio. The first effect can only explain a relatively small change in sensitivity [17,19,20,23,24]. For our measured species, the maximum differences in rate coefficients are reported for the detection of SO_2, which reacts 2.7 times faster with $CO_3^-(H_2O)$ than with $CO_3^-(H_2O)_5$, whereas the observed differences in sensitivity can be in the order of a magnitude. From this we conclude, that the effects of reverse reactions dominate the humidity dependent sensitivity.

To simplify the discussion, the effect of reverse reactions is demonstrated for the example of acetone, i.e., for Eq. (3) and its reverse reaction:

$$H_3O^+(H_2O)_n + CH_3COCH_3 \rightleftarrows H^+CH_3COCH_3(H_2O)_n + H_2O \quad (6)$$

There exist reaction cycles such as Eqs. (7)–(9), whose net reaction equals Eq. (6).

$$H_3O^+(H_2O)_n + M \rightleftarrows H_3O^+(H_2O)_{n-1} + H_2O + M \quad (7)$$

$$H_3O^+(H_2O)_{n-1} + CH_3COCH_3 \rightleftarrows H^+CH_3COCH_3(H_2O)_{n-1} + H_2O \quad (8)$$

$$H^+CH_3COCH_3(H_2O)_{n-1} + H_2O + M \rightleftarrows H^+CH_3COCH_3(H_2O)_n + M \quad (9)$$

If more complex pathways such as Eqs. (7)–(9) are ignored and only Eq. (6) is taken into account, then the equilibrium constant for Eq. (6), K_n, can be expressed as

$$K_n = \frac{k_f}{k_b} \quad (10)$$

with k_f being the rate coefficient for the forward reaction, k_b the one for the reverse reaction. K_n can also be expressed by Eq. (11):

$$K_n = e^{(-\Delta G_n^0/RT)} \quad (11)$$

where R is the universal gas constant, T the absolute temperature, and ΔG_n^0 the standard reaction Gibbs function for Eq. (6). ΔG_n^0 for $n \geq 1$ is

Table 1
Rate coefficients, k_b, for the reverse reaction of Eq. (6) (see text), estimated from the rate coefficient of the forward reaction and thermodynamical data[a]

n	ΔG_n at 80 °C, kJ mol^{-1}	K_n	k_b, cm^{-3} s^{-1}	Lifetime[b] of $H^+CH_3COCH_3(H_2O)_n$, (s)
0	122.1	1.2×10^{18}	1.6×10^{-27}	283
1	68.0	1.2×10^{10}	1.6×10^{-19}	89
2	40.2	8.8×10^{5}	2.1×10^{-15}	6.8×10^{-3}
3	31.7	4.8×10^{4}	3.8×10^{-14}	3.8×10^{-4}
4	29.1	2.0×10^{4}	9.3×10^{-14}	1.5×10^{-4}
5	27.8	1.3×10^{4}	1.4×10^{-13}	1.0×10^{-4}

[a]Calculated with data from Hunter and Lias [25] and Keesee and Castleman [26]
[b]With respect to reverse reaction according to Eq. (6) at 1% water mixing ratio, 280 hPa.

given by

$$\Delta G_n^0 = \Delta G_{n-1}^0 + \Delta G_{hyd(n-1\rightarrow n)}^0(H^+CH_3COCH_3) - \Delta G_{hyd(n-1\rightarrow n)}^0(H_3O^+) \quad (12)$$

Here, ΔG_0^0 is the difference in gas-phase basicity of acetone and water, $\Delta G_{hyd(n-1\rightarrow n)}^0$ is the Gibbs function for the hydration of a water molecule to a cluster with $n-1$ water molecules. With Eqs. (10)–(12) and the thermodynamical data from Hunter and Lias [25] and Keesee and Castleman [26], one can calculate k_b. The results are given in Table 1. They are approximate, since more complicated pathways such as Eqs. (7)–(9) were ignored and because the large uncertainties in the thermodynamic data are amplified in the exponential law Eq. (11). However, these data are well-suited to discuss the effect of reverse reactions. The rate coefficients for the reverse reaction of Eq. (6) with $n = 0$, 1 or 2 are so small that $H^+(CH_3COCH_3)$ has a lifetime with respect to the reverse reaction much longer than the reaction time of our instrument. This means, under very dry conditions, where the small clusters dominate, the reverse reaction can be neglected. However, under humid conditions, the larger clusters will dominate and the lifetime of protonated acetone clusters is in the order of the reaction time. Therefore, under more humid conditions, reactant ions and product ions can be expected to be in thermodynamical equilibrium, which is largely influenced by the water mixing ratio. Similar observations, showing that the reactions in an AP-CIMS system can be either kinetically or thermodynamically controlled, have been described by Sunner et al. [22]. They made experiments at relatively humid conditions and found ion–molecule reactions involving $H_3O^+(H_2O)_n$ ions and analytes with gas-phase basicities larger than ~800 kJ mol^{-1} to be kinetically controlled, whereas reactions with other analytes were thermodynamically controlled.

To measure traces gases with the AP-CIMS, the humidity-dependent sensitivity has to be accounted for. It has turned out to be a good solution to employ the AP-CIMS itself to determine humidity by looking at count rates of ions whose formation depends on humidity. In addition to avoiding the usage of a separate instrument for humidity measurements, this method has the advantage that humidity is measured exactly at the relevant place, that is to say in the reaction chamber of the instrument.

For positive ion spectra, the count rate ratio of different water cluster ions proved practical, e.g., the count rate ratios of the ions $H_3O^+(H_2O)_2$ or $H_3O^+(H_2O)$ to the bare H_3O^+ ion. In negative ion spectra, the ions OH^- and HCO_4^- are well suited. Which of these ions is preferable depends on the conditions in the decluster chamber. Our laboratory experiments with variable voltages on the decluster lens showed that the usage of the OH^- ions is preferable at high voltages, at which dissociation suppresses the occurrence of HCO_4^- ions. Fig. 4 shows a comparison of the humidity time series obtained with a Lyman α hygrometer and the AP-CIMS system. In this example, the AP-CIMS measurements are based upon the count

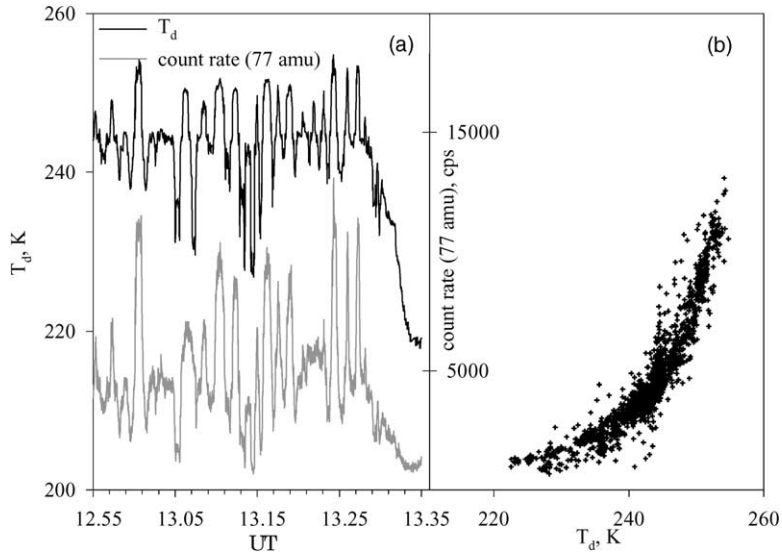

Fig. 4. (a) Comparison of the humidity time series obtained with a Lyman α absorption hygrometer (dew point temperature, black line, left axis) and the AP-CIMS (count rate 77 amu, gray line, right axis). The measurements were made on a research flight over Scandinavia on 14 October 1999. Between 1306 and 1307 UT and 1321 and 1323 UT, zero air measurements were performed which disturbed the otherwise good correlation because the zero air filter averaged the humidity the AP-CIMS was exposed to. (b) Correlation plot of dew point temperature obtained with the Lyman α absorption hygrometer versus the AP-CIMS count rate on mass 77 amu for the same period as shown in Fig. 4a, but omitting the periods when zero air measurements were performed.

rates of the HCO_4^- ions on mass 77 amu. The measurements were performed during the passage of a lee wave train, which is reflected in the large and regular changes in humidity.

Fig. 5 shows laboratory measurements of the calibration factors for acetonitrile and acetone with fit curves. Similarly, Fig. 6 shows calibration curves for sulfur dioxide. One was obtained in the laboratory, the other on a research flight over the South Atlantic and Namibia, where large differences occurred between the humid marine boundary layer on the one hand and the dry continental boundary layer and free troposphere on the other hand.

An interesting feature is that the sensitivity function of sulfur dioxide does not depend monotonously on humidity. In the curve obtained in the field, a maximum is passed and the sensitivity decreases again slightly when very dry air is probed. This behavior can be explained if one assumes that under dry conditions, Eq. (4) is kinetically controlled, since Seeley et al. [20] found a maximum of the rate coefficient for the reaction of SO_2 with $CO_3^-(H_2O)_n$ with n=1 (see Table 2). If it becomes so dry that the CO_3^- ion is favored in the source region rather than the $CO_3^-(H_2O)$ ion, exactly this behavior can be expected. At higher humidities and, therefore, in the presence of larger cluster ions, Eq. (4) becomes thermodynamically controlled, as can be assessed from the changes in sensitivity too large to be explained solely by kinetics. Thus, the case with Eq. (4) and the SO_2 detection seems to be comparable to the case with Eq. (6) and the acetone detection.

Table 2
Kinetic data for the reaction $CO_3^-(H_2O)_n + SO_2 \rightarrow CO_2 + (n - m)H_2O + SO_3^-(H_2O)_m$ (from Seeley et al. [20])

n	K_n, 10^{-9} cm^{-3} s^{-1} (T = 158 K)
0	0.88
1	1.65
2	1.59
3	1.31
4	0.86
5	0.62

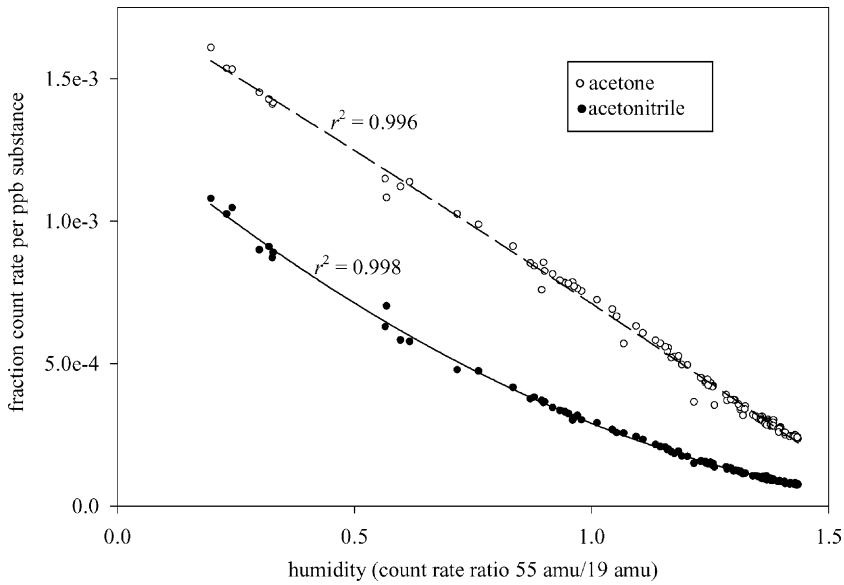

Fig. 5. Calibration curves for acetonitrile and acetone, obtained in the laboratory.

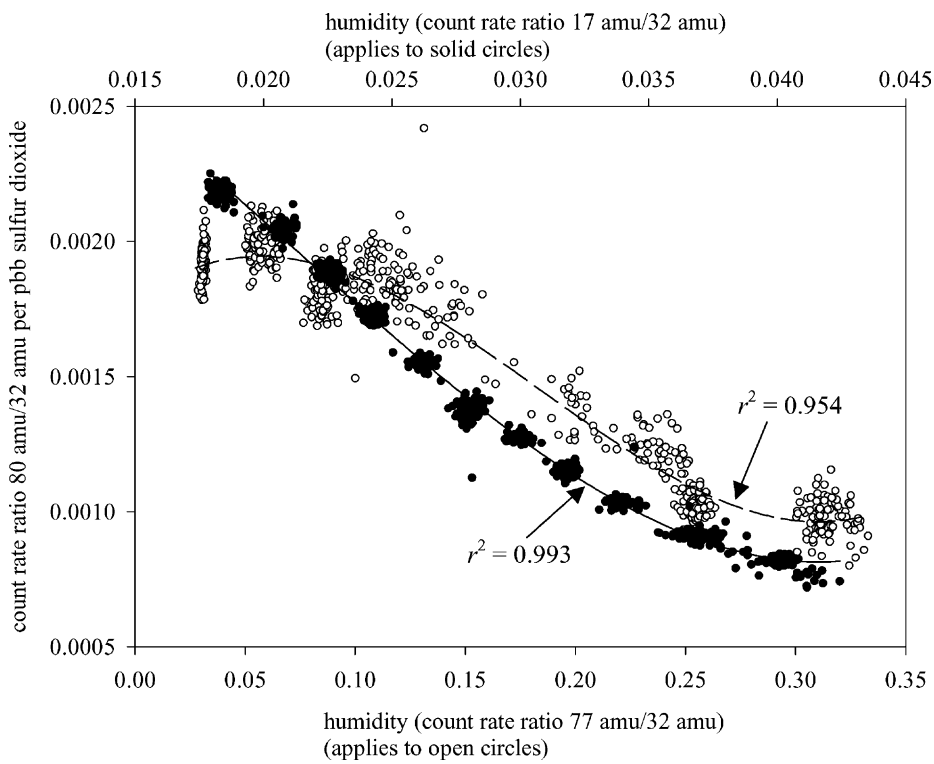

Fig. 6. Calibration curves for sulfur dioxide, obtained in the laboratory (filled circles) and in the field (open circles), obtained on a research flight over Namibia and the South Atlantic Ocean on 14 September 2000.

Obviously, the calibration curves obtained in the field show more scatter than those obtained in the laboratory. This is very likely due to fluctuations in the temperature of the probed air. The air cannot reach equilibrium with the temperature of the ion source region during the period of about 1 s spent in the heated area. The reaction rates of ion–molecule reactions can show a temperature dependence [17], and the thermodynamical equilibrium is also influenced by temperature [23].

Under dry conditions, the instrument can be used for methanol measurements as H^+CH_3OH. This was done on several research flights over Namibia [27]. However, methanol has a lower gas-phase basicity than acetone and acetonitrile and is a borderline case. The sensitivity decreases rapidly for slightly higher humidity, which limits the applicability of our instrument for this compound.

3.3. Accuracy and precision

The accuracy of the calibration system is ∼7%, with the largest contribution due to unspecific fluctuation of the permeation rates of the permeation tube, and a smaller one due to the instability of the permeation oven temperature. When performing a calibration, the calibration gas is added to the sampling line. The calculated mixing ratio of the compounds to be calibrated depends on the flow in the sampling line. From this, another error of ∼4% arises, since flow meters suffer a temperature dependency, which is especially noticeable on aircraft campaigns, where during short periods air masses of very different temperatures are to be probed.

Our method to account for sensitivity changes due to clustering allows us to perform measurements in the lower troposphere, where the humidity is high and very variable. However, the scatter in the calibration curves obtained in the field implies an error of ∼10% (see Fig. 6). This is probably the result of temperature deviations of the probed air.

The count rate statistics can cause an error. The standard deviation of statistical noise is $\sqrt{n}$, where n is the number of counts acquired per data point. Theoretically, the problem is more complex, since the mixing ratios are obtained from count rate ratios. However, the reactant ions have count rates so high that their statistical errors play a negligible role. For fairly clean conditions with typical mixing ratios of acetonitrile, acetone, and sulfur dioxide of ∼150, 1000, and 100 ppt (calculated with a typical sensitivity of 1 count per second and ppt), the statistical error is 8, 3, and 10%, respectively, for integration times of 1 s. Under these conditions, it is appropriate to prolong the integration time even on aircraft campaigns, where temporal resolution is associated with spatial resolution. The statistical error is proportional to $t^{-1/2}$ with t being the integration time.

The instrument shows blanks. For acetonitrile and acetone, the blank signals are determined using a heated catalyst, which is purged with nitrogen when not in use. The blank stems most likely from a memory effect of the inlet system. The variability of the blank of typically 10 ppt for acetonitrile and 80 ppt for acetone is the detection limit of the instrument. For sulfur dioxide, a blank variability of 20 ppt was observed for measurements outside the marine boundary layer. Zero air measurements are performed with a basic impregnated paper filter. Sodium hydroxide as the impregnator gave good results.

An overview on the precision is given in Table 3. The statistical error, which is dependent on the abundant mixing ratio and the used integration time, is not taken into account. The relative significance of the blank signal is based on the assumption of fairly clean conditions; typical mixing ratios are given.

3.4. Possible interferences

Another source of error, which, however, is difficult to quantify, is that of mass interference. Acetonitrile is detected on mass 42 amu. It is hard to think of another ion that could interfere on this low mass, especially when one takes into account that a protonated ion with an even mass number has to contain a nitrogen atom with its odd valence number. The only possible compound is the isomeric isocyano-methane, which has a gas-phase basicity of 807 kJ mol^{-1} [25], high enough

Table 3
Errors of the AP-CIMS system and their relative importance

Error source	Acetonitrile (150 ppt)	Acetone (1000 ppt)	Sulfur dioxide (150 ppt)
Non linearity (%)	<1	<1	1
Flow rate sampling line (%)	4	4	4
Calibration gas (%)	7	7	7
Scatter in calibration curve (%)	10	10	10
Variability of blank (%)	7	8	13
Overall (%)	15	15	18

so that it could be detected. Fragmentation studies [18] suggest that the mass signal at 42 amu originates uniquely from acetonitrile, which means that the atmospheric concentration of isocyano-methane is negligible. However, the finding of the negligible isocyano-methane mixing ratios in sporadic studies does not exclude atmospheric sources of this compound, assumed that its lifetime is too short to be present in significant amounts distant from its sources. Then, acetonitrile measurements near isocyano-methane source could suffer an interference. Another compound, 2H-azirine, plays very likely no role as an atmospheric constituent, since it is rather unstable due to its three-ring structure. A further interference can occur from compounds with the formula C_3H_4 with one ^{13}C-atom, namely propyne, propadiene, and cyclopropene, which have gas-phase basicities high enough, so that they are detectable [25]. However, the ^{13}C isotope makes up only 1.108% of all carbon, so only ∼3% of these compounds contain a ^{13}C-atom, which minimizes the interference.

Acetone is detected as the $H^+(CH_3COCH_3)$ ion on mass 59 amu. Other candidates for this mass are several isomeric compounds such as propanaldehyde (CH_3CH_3CHO), methyl ethyl ether, various propenols, and some cyclic ethers and alcohols. Furthermore, there exists a variety of compounds not isomeric to acetone, but with roughly the same mass, which would not be distinguishable from acetone molecules with a quadrupole mass filter of the kind used. Further compounds containing heavy isotopes can interfere, but as in the case of acetonitrile, the significance is low due to the low abundance of the heavy isotopes.

Reiner et al. [18] showed by atmospheric dissociation studies based on background air measurement that mass 59 amu in general stems uniquely from acetone. Williams et al. [28] conclude the same from evaluating variability–lifetime relationships. However, as in the case for acetonitrile, one can argue that these tests are only valid for source distant background air. If a compound is released in substantial amounts to the atmosphere, but is too short-lived to be measurable distant from its source, measurements of acetone close to these sources could overestimate acetone.

Mass 80 amu (SO_3^-) used for the SO_2 detection can also stem from $NO_3(H_2O)^-$, but its presence could be ruled out after adjusting the conditions in the decluster chamber. No other ion is expected to cause an interference on this mass. However, it was surprisingly found that dimethylsulfide and methyl mercaptan account for a sulfur dioxide signal with a comparable sensitivity as sulfur dioxide itself. Likely, it is due to the fast decomposition of these compounds by the radicals produced in the corona discharge, causing formation of SO_3^-. This view is supported by the finding that the compounds causing problems are those reduced sulfur compounds with the shortest atmospheric lifetime with respect to radical reactions [29], whereas other sulfur compounds such as hydrogen sulfide, carbon disulfide, carbonyl sulfide, methane sulfonic acid, and sulfuric acid do not cause an effect.

This finding suggests that AP-CIMS with a corona discharge as ion source could be inappropriate for the detection of sulfur dioxide in the marine boundary layer, where high and variable mixing ratios of dimethylsulfide and, to a lesser extent, methyl mercaptan are to be expected (e.g., [30] and references

therein). If the mixing ratios of these compounds are constant, they do not cause a problem, because then, their influence is accounted for in the zero air measurements (see Section 3.3).

4. Conclusions and plans

We have set up an AP-CIMS for fast measurements of acetonitrile, acetone, and sulfur dioxide. A corona discharge is used as ion source. Acetonitrile and acetone are detected as protonated species in the positive ion mode and can be monitored simultaneously. Sulfur dioxide can be monitored in the negative ion mode, where it causes a signal of SO_3^- ions.

The problem of clustering that can cause the sensitivity of an AP-CIMS to be dependent on the humidity of the sample gas was solved with a novel method. The method is based on determining a humidity dependent calibration curve. It could be shown that the mass spectrometer itself can be used to measure the humidity. This way, one is able to perform fast measurements of the humidity in the ion–molecule reaction chamber without employing additional instruments.

The detection limits are between 10 and 80 ppt for the different species. The precisions of the measurements are 18% or better under typical conditions if an appropriate integration time is used to minimize statistical errors. An appropriate integration time in this sense is 3 s under typical conditions. The actual measurement frequency is lower, because also the reactant ions of the involved ion–molecule reactions and the ions to determine the humidity of the sample have to be monitored. The measurement frequency is also influenced by the number of species monitored. In several aircraft campaigns, an effective measurement frequency of 1 in 15 s after averaging has proven to be appropriate. Under special circumstances, such as strong pollution near sources, a measurement frequency of 1 in 1 s is possible. The instrument is a good tool to determine concentrations of atmospheric trace gases, especially in situations where a fast technique is necessary, i.e., for airborne measurements or eddy-correlation measurements [12]. Beside humidity, the temperature of the sample gas in the ion–molecule reaction volume influences clustering and, thus, the sensitivity. With the current set-up, the temperature may be slightly variable under certain field conditions. This could be improved by pre-warming the sample gas before it enters the ion–molecule reaction region to achieve a better precision of the instrument.

It turned out that the radicals produced in the corona discharge cause interferences with dimethylsulfide and methyl mercaptan when measuring sulfur dioxide. An ion source based on a radioactive substance instead of a corona discharge to produce fewer radicals is not a good solution for an instrument employed in international campaigns because of safety regulations. Berresheim et al. [9] report on the addition of propane as a radical scavenger to prevent HO measurements by AP-CIMS from suffering artifacts from radicals produced in the ion source. This could be a method to dispose of the interferences from reduced sulfur compounds in our future sulfur dioxide measurements.

Acknowledgements

We thank the staff of the Meteorological Research Flight of the UK Met Office. Ken Dewey provided the Lyman α hygrometer data. We also thank the staff of the US NCAR-RAF C-130. We thank Meinrat O. Andreae for the support of our work in the framework of the various campaigns. We are grateful to Martin Vollmer and Carol Strametz for useful comments and corrections. We strained the helpfulness of Frank Helleis and Michael Flanz from the electronics department, especially shortly before the campaigns. Financial support from the Max Planck Society and the European Commission is gratefully acknowledged.

References

[1] F. Arnold, D. Krankowsky, K.H. Marien, Nature 267 (1977) 30.
[2] F.L. Eisele, Int. J. Mass Spectrom. Ion Processes 54 (1983) 119.
[3] G. Knop, F. Arnold, Planet. Space Sci. 33 (1985) 983.
[4] F.L. Eisele, H. Berresheim, Anal. Chem. 64 (1992) 283.

[5] H. Berresheim, D.J. Tanner, F.L. Eisele, Anal. Chem. 65 (1993) 84.
[6] H. Berresheim, D.J. Tanner, F.L. Eisele, Anal Chem. 65 (1993) 3168.
[7] F. Arnold, J. Schneider, K. Gollinger, H. Schlager, P. Schulte, D.E. Hagen, P.D. Whitefield, P. van Velthofen, Geophys. Res. Lett. 23 (1997) 57.
[8] T. Reiner, M. Hanke, F. Arnold, H. Ziereis, H. Schlager, W. Junkermann, J. Geophys. Res. 104 (1999) 18647.
[9] H. Berresheim, T. Elste, C. Plass-Dülmer, F.L. Eisele, D.J. Tanner, Int. J. Mass Spectrom. 202 (2000) 91.
[10] T. Reiner, D. Sprung, C. Jost, R. Gabriel, O.L. Mayol-Bracero, M.O. Andreae, T.L. Campos, R.E. Shetter, J. Geophys. Res. 106 (2001) 28497.
[11] D. Sprung, C. Jost, T. Reiner, A. Hansel, A. Wisthaler, J. Geophys. Res. 106 (2001) 28511.
[12] D. Sprung, PhD thesis, Brandenburg Technical University, Cottbus, 2001.
[13] P.R. Field, R.J. Cotton, K. Noone, P. Glantz, P.H. Kaye, E. Hirst, R.S. Greenway, C. Jost, R. Gabriel, T. Reiner, M. Andreae, C.P.R. Saunders, A. Archer, T. Choularton, M. Smith, B. Brooks, C. Hoell, D. Johnson, A. Heymsfield, Q. J. R. Meteorol. Soc. 127 (2001) 1493.
[14] C. Jost, paper in preparation.
[15] C. Jost, J. Trentmann, D. Sprung, M. O. Andreae, J. B. McQuaid, H. Barjat, J. Geophys. Res., in press.
[16] A. A. Viggiano, F. Arnold, in: H. Volland, (Ed.), Handbook of atmospheric Electrodynamics, I, CRC, Boca Raton, 1995, p. 1.
[17] A.A. Viggiano, F. Dale, J.F. Paulson, J. Chem. Phys. 88 (1988) 2469.
[18] T. Reiner, O. Möhler, F. Arnold, J. Geophys. Res. 103 (1998) 31309.
[19] O. Möhler, T. Reiner, F. Arnold, J. Chem. Phys. 97 (1992) 8233.
[20] J.V. Seeley, R.A. Morris, A.A. Viggiano, Geophys. Res. Lett. 23 (1997) 1379.
[21] H. Kambara, I. Kanomata, Int. J. Mass. Spectrom. Ion Phys. 25 (1977) 129.
[22] J. Sunner, G. Nicol, P. Kebarle, Anal. Chem. 60 (1988) 1300.
[23] J. Sunner, M.G. Ikonomou, P. Kebarle, Anal. Chem. 60 (1988) 1308.
[24] G. Nicol, J. Sunner, P. Kebarle, Int. J. Mass. Spectrom. Ion Phys. 84 (1988) 135.
[25] E.P. Hunter, S.G. Lias, J. Phys. Chem. Ref. Data 27 (1998) 413.
[26] R.G. Keesee, A.W. Castleman, J. Phys. Chem. Ref. Data 15 (1986) 1011.
[27] C. Jost, PhD thesis, Ruperto-Carola-University, Heidelberg, 2002.
[28] J. Williams, H. Fischer, G.W. Harrias, P.J. Crutzen, P. Hoor, A. Hansel, R. Holzinger, C. Warneke, W. Lindinger, B. Scheeren, J. Lelieveld, J. Geophys. Res. 105 (2000) 20473.
[29] R. Atkinson, D.J. Baulch, R.A. Cox, R.F. Hampson Jr, J.A. Kerr, J.A. Rossi, J. Troe, J. Phys. Chem. Ref. Data 26 (1997) 521.
[30] A.J. Kettle, T.S. Rhee, M. von Hobe, A. Poulton, J. Aiken, M.O. Andreae, J. Geophys. Res. 106 (2001) 193.